

Kinetically-decoupled electrical and structural phase transitions in VO₂S. R. Sahu,¹ S. S. Majid,^{2,3} A. Ahad,^{4,*} A. Tripathy,¹ K. Dey,¹ S. Pal,¹ B. K. De,¹
Wen-Pin Hsieh,² R. Rawat,¹ V. G. Sathe,¹ and D. K. Shukla^{1,†}¹*UGC-DAE Consortium for Scientific Research, Indore-452001, India*²*Institute of Earth Sciences, Academia Sinica, Nankang, Taipei-11529, Taiwan*³*Department of Physics, National Institute of Technology Hazratbal Srinagar J & K-190006, India*⁴*New chemistry unit (NCU), Jawaharlal Nehru Center for advanced Scientific Research Bangalore-560064, India*

(Received 11 December 2022; revised 15 March 2023; accepted 17 March 2023; published 7 April 2023)

Vanadium dioxide (VO₂) has drawn significant attention for its near room temperature insulator-to-metal transition and associated structural phase transition. The underlying Physics behind the temperature induced insulator-to-metal and concomitant structural phase transition in VO₂ is yet to be fully understood. We have investigated the kinetics of the phase transitions of VO₂ with the help of resistivity measurements and Raman spectroscopy. Resistance thermal hysteresis scaling and relaxation measurements across the temperature induced insulator-to-metal transition reveal an unusual behavior of this first-order phase transition, whereas relaxation phenomena investigated by Raman spectroscopy show that the temperature induced monoclinic to rutile phase transition in VO₂ follows usual behavior and is consistent with mean field prediction. Insulator-to-metal and structural phase transitions have been found to decouple with an increased temperature sweep rate. The observed unusual thermal hysteresis scaling behavior with temperature sweep rate during insulator-to-metal transition may be the consequences of independent diffusion of charge and heat due to unconventional quasiparticle dynamics in VO₂. Unconventional quasi particle dynamics, i.e., significantly lowered electronic thermal conductivity across insulator-to-metal transition in our sample is verified by ultrafast optical pump-probe time domain thermoreflectance measurements.

DOI: [10.1103/PhysRevB.107.134106](https://doi.org/10.1103/PhysRevB.107.134106)**I. INTRODUCTION**

VO₂ undergoes a first-order insulator-metal transition (IMT) at a critical temperature ($T_c \approx 340$ K) at ambient pressure and is accompanied by structural change from the monoclinic insulating phase (M1: $P2_1/c$) into the rutile metallic phase (R: $P4_2/mnm$) [1–4]. Nature of this phase transition has been discussed controversially in literature, whether it is lattice distortion driven Peierls transition or electron correlation driven Mott transition [5]. The near room temperature insulator-to-metal transition of VO₂ is extremely interesting for various important applications such as in Mott memory, Mott FET, neuromorphic devices, and more [6–8]. Therefore, better insights about the first-order phase transition behavior of VO₂ is pivotal from both fundamental physics and application points. This has motivated researchers to investigate the coupling/decoupling of above transitions through external stimuli such as light [2,9], strain [10–12], and charge injection [13,14].

The first-order phase transition (FOPT) is not an instantaneous phenomenon but it is a dynamic process, and the nucleation and growth have their own kinetics [15]. FOPT commonly occurs under heating or cooling cycles, exhibits hysteresis across the transition, and is accompanied by sharp

discontinuities in physical properties such as resistance. In FOPT, conversion from phase-1 (parent phase) to phase-2 (daughter phase) will proceed over a finite time even after the control parameter (T , in the case of temperature induced FOPT) has reached its value (T_c , defined by average of the transition temperature of the heating and cooling cycles), which leads to a phase coexistence [15]. The phenomenon of phase coexistence is broadly observed across a large number of condensed matter systems, such as high- T_c superconducting cuprates [16,17], colossal magneto resistive manganites [18–20], and in Vanadium oxides [3,21–24].

During FOPT, nuclei formation of the daughter phase within the parent phase is known as the nucleation phenomenon, and subsequent diffusion is the mechanism that guides and determines the phase transformation kinetics and is governed by mean field predictions. Earlier reports suggest that thermal scaling of hysteresis and relaxation measurements are key experiments to test the mean field predictions during FOPT [25–28]. As per mean field prediction, critical-like slowing down of phase transformation would be observed around the transition if the system approaches a genuine bifurcation point. A systematic delay is observed in the onset temperature which is dependent on the temperature sweeping rate (TSR) [25,29–31]. Such systematic delay in the onset of phase switching is predicted and observed in various physical systems in a definite scaling form [29,30]. Rising area of the hysteresis loop with increasing driving force sweeping rate has been theoretically predicted as well as experimentally observed in V₂O₃ [25,32,33].

*Present Address: School of Physical and Mathematical Sciences, Nanyang Technological University, Singapore.

†Corresponding author: dkshukla@csr.res.in

Here, we have experimentally studied the kinetics of thermally induced FOPT in VO₂. Minor hysteresis loop (MHL) in resistivity measurement confirmed the presence of phase-coexistence during phase transition in VO₂. The thermal hysteresis in resistivity measurements have been found to shrink with increasing TSR which is in contrast to the conventional FOPT.

Observed unusual thermal hysteresis scaling behavior with TSR during insulator-to-metal transition may be the consequences of independent diffusion of charge and heat due to unconventional quasiparticle dynamics in VO₂. To substantiate the claim of unconventional quasiparticle dynamics we have also performed the temperature dependent thermal conductivity measurements which clearly indicates the significantly lower electronic thermal conductivity across insulator-metal transition in the studied VO₂ thin film.

II. EXPERIMENTS

The VO₂ thin film used in this study is grown on r-cut Al₂O₃ substrate using pulsed laser deposition technique. A KrF excimer laser, $\lambda = 248$ nm, repetition rate of 5 Hz and pulse energy of 370 mJ, was focused onto the V₂O₅ target with a fluence of ~ 1.1 J/cm². During deposition, ultrasonically cleaned r-cut Al₂O₃ substrate was maintained at a temperature of $\sim 700^\circ\text{C}$ and oxygen partial pressure was maintained at ~ 10 mTorr. Prior to the gas introduction, chamber was pumped down to base pressure of 1×10^{-6} Torr. Bruker D8 x-ray diffractometer with Cu K α radiation was used for x-ray diffraction (XRD) measurement. Electrical transport measurement has been performed in linear four point probe configuration using Keithley 2401 source meter and Keithley 2182A nanovoltmeter. Temperature was controlled using the Cryocon 22C temperature controller. Raman spectroscopy is carried out in back scattering geometry using the 8 mW Ar (473 nm) laser as an excitation source coupled with a Labram-HR800 micro-Raman spectrometer. X-ray absorption spectra (XAS) across V L_{2,3} edge and O-K edge has been measured in total electron yield mode at SXAS beamline BL-01 of Indus-2 at RRCAT, Indore, India. Room temperature XRD Fig. S1(a) and Raman spectra Fig. S1(b) confirmed the monoclinic *M1* phase in the VO₂ thin film [5,34]. Phase purity and spatial homogeneity has been confirmed by XAS and Raman mapping over an area of $30 \times 30 \mu\text{m}^2$, see Supplemental Material [35] (see also references [36–47] therein). Several orders of magnitude change in resistivity across the IMT reflects the high crystalline quality of the VO₂ thin film, Fig. S1(c). In order to completely characterize the IMT, transition temperature (T_c) and hysteresis width (ΔH) is calculated from the Gaussian fitting of the differential curve of $\ln R$ vs T plot. ΔH defined as the difference in the transition temperature for heating and cooling and T_c is defined by the average of the transition temperatures of the heating and cooling cycle.

III. RESULTS

First, we have evaluated the first-order characters of the phase transition in the pulsed laser deposition grown VO₂ thin film. Resistivity measurement showed several orders of change in resistance magnitude and hysteresis across

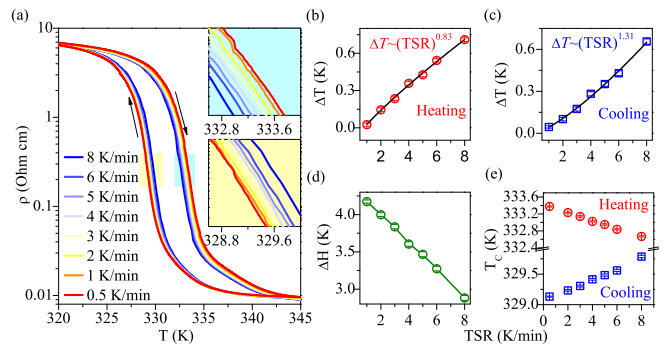


FIG. 1. Thermal hysteresis scaling. (a) Temperature sweeping rate dependent resistivity measurements of VO₂, arrows indicate heating and cooling cycle data across T_c . Insets show enlarged views of heating and cooling cycle data across T_c . (b) and (c) show fittings of shifts in transition temperatures ($\Delta T = |T_c - T_o|$) with varying TSR in heating and cooling cycles, respectively. Hysteresis width (ΔH) and transition temperature (T_c) variations as a function of TSR are presented in (d) and (e), respectively, (see text for detail).

transition which confirmed FOPT character [see Fig. S1(c)]. On a well characterized thin film we have performed the temperature sweeping rate dependent measurements to test the mean field predictions. Resistivity relaxation measurement in the phase coexistence region has been used to track the time evolution of grown metallic phase and the Raman spectroscopy relaxation measurement is used to track the time evolution of the rutile structure. The combined results of the above discussed experimental protocols have been utilized to understand the enigma of observed anomalous FOPT.

(i) *Thermal hysteresis scaling.* The dynamic hysteresis loop in Fig. 1(a) shows the temperature dependent resistivity of the VO₂ thin film in the heating and cooling cycles for different TSR, ranging between 0.5 K/min and 8 K/min. Zoomed view of hysteresis loops in heating and cooling cycles are shown in insets. The shape of hysteresis loops is sensitive to the phase transformation rate [48]. We observed a systematic shrinking of the hysteresis width with increasing TSR, which is unusual for FOPT. A standard way to depict the dynamic shift is to plot the rate dependence of dynamical renormalization shift $\Delta T(R)$. We have plotted the variation of the dynamical renormalization shift of the transition temperature with TSR for heating [Fig. 1(b)] and cooling [Fig. 1(c)] cycles. Dynamical renormalization shift ΔT is defined by $\Delta T = |T_{hc} - T_o|$, where T_{hc} is the transition temperature of the corresponding resistivity curves for heating and cooling cycles performed at a particular TSR and T_o is the transition temperature of the quasistatic resistivity curve for heating and cooling cycles. The slowest rate here, i.e., 0.5 K/min, has been considered as a quasistatic case for calculations and obtained T_o are 333.38 K and 329.13 K for heating and cooling cycles, respectively. The change in the area of the hysteresis loop (or equivalently, the shift in the transition point) can be scaled with a sweeping rate (rate of change of temperature T as a power law) [33,49,50]. The ΔT vs TSR data has been successfully fitted by the expression $\Delta T \sim (TSR)^\gamma$ and the values of gamma for the heating and cooling cycles have been obtained by fitting as 0.83 ± 0.07 and 1.31 ± 0.10 [see Figs. 1(b) and 1(c)].

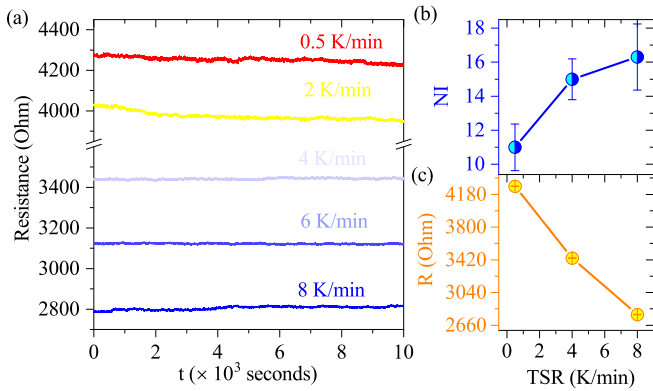


FIG. 2. (a) Resistance relaxation measurements performed at 332 K (T_m) for different TSR. (b) shows the strengthening of normalized Raman intensities (NI) and (c) decreasing resistance values with increasing TSR at T_m , i.e., decreased insulating character but increased monoclinic phase fraction with TSR.

Variations of the hysteresis width (ΔH) and transition temperatures (in heating and cooling cycles) with varying TSR are shown in Figs. 1(d) and 1(e), respectively. Although these results show the strong TSR dependence of the IMT, the trend is opposite to the usual FOPT character [25,28].

(ii) *Resistivity relaxation measurements.* To monitor the time evolution of the metallic phase we have collected the resistance data at constant temperature $T_m \sim 332$ K [marked by the dashed line in the inset of Fig. S1(c)] for around $\sim 10\,000$ seconds for each TSR. For the relaxation measurement, one needs a temperature in the phase coexistence region where nucleation of the metallic phase has started. Therefore, T_m is chosen in the middle of the phase transition [26,51]. The protocol we have used for the relaxation measurement is as follows. Each measurement starts from the same initial temperature in insulating phase (i.e., 280 K) but with different TSRs (0.5–8 K/min). For each TSR, as soon as T_m (measurement temperature) is approached, the resistance is measured for $\sim 10\,000$ seconds. After, each time dependent resistance measurement sample is cooled again to the initial temperature. It is clearly observed that the trend of the relaxation data is not as that predicted by usual FOPT [Fig. 2(a)]. For each TSR, resistance value has been observed to be almost constant all through the time evolution which is unusual. According to the usual FOPT behavior, if one stops the transition driving force in the transition region (which is temperature here) and leaves it for time evolution, then the system always has (whatever be the TSR) a tendency to go to the daughter phase [26].

(iii) *Raman relaxation measurements.* Raman spectroscopy is highly sensitive to the changes in vibrational modes and hence, is a powerful tool for the investigations of structural and chemical transformations in organic and inorganic materials induced by temperature, pressure, doping etc., [52–56]. Subtle changes in the V-V dimers of VO_2 leads to temperature induced monoclinic to rutile phase transformation. This phase transition has been extensively studied by Raman spectroscopy [5,34,57–59]. According to group theory, the $M1$ phase of VO_2 has 18 Raman active modes (9Ag and 9Bg), out of which 12 modes at $\sim 138, 193, 223, 261, 308, 338, 387, 439, 442, 498, 583,$ and 613 cm^{-1} [34] are observed in

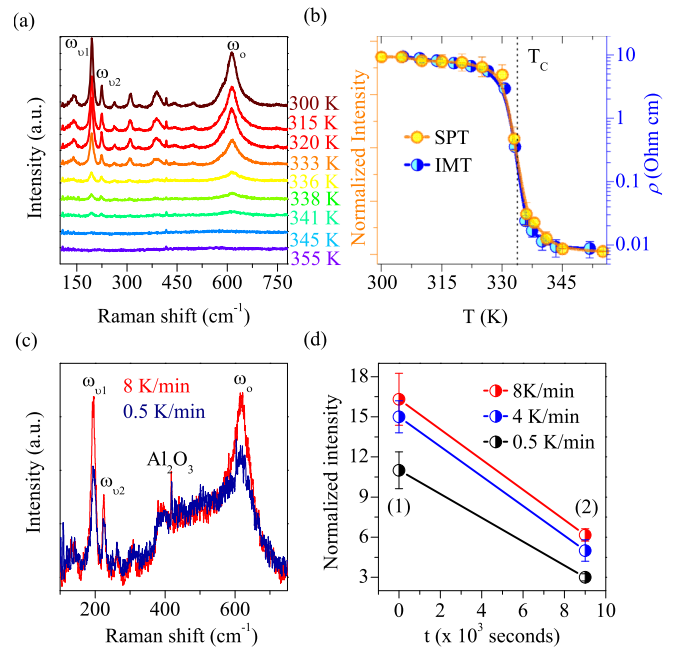


FIG. 3. (a) Temperature dependent Raman spectra where disappearance of Raman modes with increasing temperature confirms transition from monoclinic phase to rutile phase. (b) Plot of insulator-metal transition from temperature dependent resistivity data and temperature induced monoclinic to rutile structural phase transition from Raman data, both measured at 2 K/min. Dashed vertical line denotes the T_c (c) Raman spectra collected immediately at T_m after reaching to this temperature with slowest (0.5 K/min) and fastest (8 K/min) TSR. (d) Normalized intensity vs time, where data points (1) represent the Raman intensity at $t = 0$ (measured immediately after reaching at 332 K) and data point (2) represent the Raman intensity after $t = 9000$ seconds for different TSR.

the VO_2 thin film, and Raman mode at $\sim 417\text{ cm}^{-1}$ belongs to the Al_2O_3 substrate [see Fig. 3(a)] [40]. The three modes labeled as ω_{v1} ($\sim 193\text{ cm}^{-1}$) and ω_{v2} ($\sim 223\text{ cm}^{-1}$), which belong to the the V-V vibrations [37], and ω_o ($\sim 615\text{ cm}^{-1}$) which represents V-O-V vibration [see Fig. S1(b)] has been treated as key modes in phase transition region studies of VO_2 [5,40]. Disappearance of Raman modes with increasing temperature signifies the monoclinic to rutile structural phase transition (SPT) [see Fig. 3(a)]. Details related to the investigations of structural transition from the monoclinic to rutile using Raman data, such as mode assignment, shift in the peak position, and FWHM of the modes with varying temperature etc., has been provided in the Supplemental Material [35] (see also Refs. [36,37,60,61] therein). At a slower temperature sweeping rate, temperature induced IMT and SPT are found to occur simultaneously, which is seen in the plot of temperature dependent resistivity and the normalized intensity of the Raman mode (ω_{v1}) of the VO_2 thin film, both measured in the heating cycle for 2 K/min TSR [see Fig. 3(b)]. To monitor the time evolution of the rutile metallic phase, Raman spectroscopy relaxation measurement is performed using the similar protocol as used for the resistivity relaxation measurements, shown in Fig. 3(d). For each TSR a Raman spectrum is measured immediately when T_m (332 K) is approached

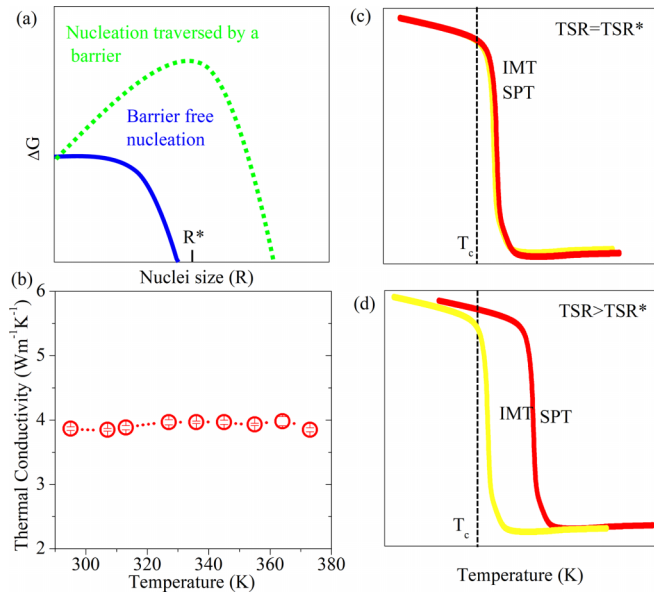


FIG. 4. (a) shows the processes of nucleation traversed through the barrier and barrier-free paths during FOPT. (b) Temperature dependent thermal conductivity data of VO₂ thin film. (c) shows that transition temperature is similar for $TSR = TSR^*$, where TSR^* is the optimum temperature sweep rate until when IMT and SPT are coupled. (d) is the case for $TSR > TSR^*$, i.e., when IMT leads by SPT because SPT is a highly time dependent process. T_c represents the transition temperatures, while IMT and SPT curves [in (c) and (d)] are representing data of heating cycles only.

[Fig. 3(c)]. Immediately measured Raman spectra are shown in Fig. 3(c) for the lowest TSR (0.5 K/min) and for highest TSR (8 K/min). It is clearly seen that Raman modes are stronger for 8 K/min TSR compared to that of 0.5 K/min (intensities are normalized by Al₂O₃ mode), which indicates larger monoclinic phase fraction for 8 K/min. This result is in contrast to the resistivity data where resistance is found consistently decreasing with increasing TSR. To compare the relaxation data of Raman spectroscopy with the resistivity relaxation data, we have fitted the most intense Raman mode ($\omega_{v1} \sim 193\text{cm}^{-1}$) with a Lorentz function and plotted the area as a function of time for different TSR [Fig. 3(d)]. Significantly decreased intensity of the Raman mode at T_m with time indicates the growth of the rutile phase for each TSR [see Fig. 3(d)], which is expected and signifies usual FOPT behavior. Figure 2(b) shows the normalized Raman intensity and Fig. 2(c) shows the trend of resistance at T_m (at $t = 0$ second) with varying TSR which clearly indicate the decoupling character of IMT and SPT with TSR.

(iv) *Thermal conductivity measurement.* Our principal experimental protocol is based on temperature sweeping rate, therefore, the thermal conductivity of the material is of paramount importance in governing the kinetics of phase transition. Thermal conductivity measurements have been performed across phase transition temperature regions in the VO₂ thin film. Thermal conductivity (Λ) has been found to be almost constant at $\sim 4 \text{ Wm}^{-1}\text{K}^{-1}$ in the measured temperature region across insulator-to-metal transition [see Fig. 4(b)]. Details of thermal conductivity measure-

ments using the time-domain thermo-reflectance method is provided in the Supplemental Material [35] (see also references [62–65] therein). Our results are consistent with the earlier report [66]. On the phase transition into the metallic phase an increase in the thermal conductivity is expected. However, no such rising thermal conductivity behavior with onset of metallicity is observed. Lee *et al.*, who also measured the thermal conductivity in VO₂ across insulator-to-metal transition, have confirmed that low electronic thermal conductivity in metallic phase is a signature of the unconventional quasiparticle dynamics, where heat and charge diffuse independently [66].

IV. DISCUSSIONS

Nucleation and growth mechanism during phase transformations in solids has been a subject of great interest [67] but it is quite difficult to get a physical parameter from bulk measurements which can be directly related to the phase evolution. Generally, hysteresis accompanied with the transition is considered as an appropriate tool to determine the first-order nature of the transition [68]. Therefore, hysteresis observed in our resistivity measurements is utilized to characterize the first-order phase transition. Moreover, phase coexistence which is a typical signature of FOPT is also observed in resistivity, as seen in the MHL measurements of the VO₂ thin film [see Fig. S1(d)] [69].

The explicit character of FOPT is that with increasing TSR hysteresis should broaden [25]. We have observed the shrinking of hysteresis with increasing TSR [Fig. 1(a)]. This is in stark contrast to FOPT character and possible only when by some means the number of nucleation centers get enhanced by rising TSR [70]. However, the situation for the SPT probed by Raman spectroscopy is found consistent with FOPT behavior. We have observed the less intense Raman modes for low TSR (0.5 K/min) compared to that of high TSR (8 K/min), at the same temperature (T_m) [Fig. 3(c)]. The observed influence of TSR on Raman data clearly hints toward broadening of the SPT hysteresis with increasing TSR which is usual. In order to clearly visualize the effect of TSR on IMT and SPT, immediately obtained values of normalized Raman intensity [Fig. 2(b)] and resistance [Fig. 2(c)] (at $T_m = 332$ K) are plotted as a function of TSR. These two data, Raman and resistivity, clearly show opposite trends. At 332 K, by increasing TSR, resistance value decreases while normalized Raman intensity increases which signifies the less insulating but more monoclinic phase fraction with TSR. The delay in SPT is obvious as it is not an instantaneous process and would require time. Our observations clearly show the decoupling of the IMT and the SPT in VO₂ with TSR. Decoupling of IMT and SPT in VO₂ has been observed earlier also by charge injection method [13].

The nonequilibrium phase fraction is related to the “degree of metastability” and for a FOPT this dictates the kinetics of the growth of the daughter phase [27]. So, the time taken for the relaxation of the nonequilibrium phase into the daughter phase depends on growth of the respective nuclei and available interface [27]. Surprisingly, we have observed that resistance is almost constant all through time evolution, which is not usual, and hints toward a barrier free nucleation type

behavior in VO₂. Present observations clearly show that the nuclei which are grown during temperature sweeping does not further grow (during time relaxation) when heat flux has stopped. Moreover, at constant temperature [at 332 K, see Fig. 2(a)] decreasing values of resistance with increasing TSR clearly indicates that with increasing TSR nucleation centers have also increased. These observations of time independent behavior of resistance and enhancement of nucleation centers with increasing TSR is the consequence of barrier free nucleation. In a barrier free nucleation, as soon as the barrier to nucleation diminishes, the nucleation process will enhance and resultant hysteresis will shrink, as observed here. Huffman *et al.* also reported the IMT through a barrier free path in VO₂ thin film [71]. Barrier free nucleation is a kind of heterogeneous nucleation and in such a case the free energy of forming the critical nucleus can be altered significantly [71]; however, in usual FOPT, homogeneous nucleation occurs only by passing through the free energy barrier (ΔG) [see Fig. 4(a)] [71–73].

On the contrary, from Raman spectroscopy relaxation measurements it is clear that normalized intensity of Raman modes are decreasing with time [Fig. 3(d)] at each TSR. These results are consistent with the mean field prediction, i.e., the monoclinic phase is going to disappear with time at T_m , as rutile phase must evolve. The observed difference in behavior of IMT and SPT could be resultant of independent diffusion of the heat and charge in the VO₂, which is supported by the temperature independence of thermal conductivity behavior in VO₂ [see Fig. 4(b)].

After all this deliberation we come to the conclusion that at smaller TSR, IMT is accompanied with SPT but beyond a critical TSR decoupling has been observed. TSR dependent decoupling of IMT and SPT has been summarized in Figs. 4(c) and 4(d) and is understood as follows. In VO₂, due to unconventional quasiparticle dynamics, charge and heat flows independently in the phase transition regime, so flow of charge, which is responsible for metallic character, will be independent from the structural transition driven by heat flow. Therefore, by increasing the TSR, VO₂ becomes metallic relatively early but does not transform into the rutile phase because structural phase transition is highly time dependent and cannot be accelerated by raising the TSR.

Further, in order to discard the contribution of strain (which is inevitable in thin film form), and to check the reliability of our results, we have also performed the TSR dependent resistivity measurements on the polycrystalline VO₂ pellet and we have observed the similar results, i.e., shrinking of hysteresis with TSR (see Fig. S5) [35]. For further consistency we have also performed similar experiments on polycrystalline V₂O₃ and found broadening of hysteresis with TSR (Fig. S6 [35]) which is in accordance to mean field prediction and similar to earlier reported data [25].

V. CONCLUSIONS

Finally, it is observed that with temperature sweeping rate, insulator-to-metal transition in VO₂ exhibits the unusual FOPT character, while structural phase transition (from monoclinic to rutile) with TSR follows usual FOPT behavior. Our results clearly show the decoupling of insulator-to-metal transition and structural phase transition beyond a critical temperature sweeping rate. Our TSR dependent and relaxation measurement of resistivity in the phase coexistence region confirms that insulator-to-metal transition in VO₂ is following the barrier free path. The unconventional quasiparticle dynamics behavior (confirmed through temperature dependent thermal conductivity measurement) in the phase transition regime is held responsible for independent diffusion of charge and heat which facilitates the decoupling of IMT and SPT. Ultimately, we come to the conclusion that unconventional quasiparticle dynamics can transcend the phase transformation kinetics in VO₂ and mean field predictions of FOPT cannot truly predict the IMT behavior, especially at higher temperature sweep rates.

ACKNOWLEDGMENTS

D.K.S. acknowledges support from SERB New Delhi, India in the form of early career research award (ECR/2017/000712). S.S.M. acknowledges the financial support from SERB, India, in the form of the national post doctoral fellowship (NPDF) award (PDF/2021/002137). Martin Greven and Damjan Pelc are gratefully acknowledged for fruitful suggestions.

-
- [1] J. Laverock, S. Kittiwatanakul, A. A. Zakharov, Y. R. Niu, B. Chen, S. A. Wolf, J. W. Lu, and K. E. Smith, Direct Observation of Decoupled Structural and Electronic Transitions and an Ambient Pressure Monocliniclike Metallic Phase of VO₂, *Phys. Rev. Lett.* **113**, 216402 (2014).
- [2] V. R. Morrison, R. P. Chatelain, K. L. Tiwari, A. Hendaoui, A. Bruhács, M. Chaker, and B. J. Siwick, A photoinduced metal-like phase of monoclinic VO₂ revealed by ultrafast electron diffraction, *Science* **346**, 445 (2014).
- [3] M. M. Qazilbash, M. Brehm, B.-G. Chae, P.-C. Ho, G. O. Andreev, B.-J. Kim, S. J. Yun, A. Balatsky, M. Maple, F. Keilmann *et al.*, Mott transition in VO₂ revealed by infrared spectroscopy and nano-imaging, *Science* **318**, 1750 (2007).
- [4] J. Nag, R. F. Haglund Jr, E. Andrew Payzant, and K. L. More, Non-congruence of thermally driven structural and electronic transitions in VO₂, *J. Appl. Phys.* **112**, 103532 (2012).
- [5] S. S. Majid, D. K. Shukla, F. Rahman, S. Khan, K. Gautam, A. Ahad, S. Francoual, R. Choudhary, V. G. Sathe, and J. Strempler, Insulator-metal transitions in the T phase Cr-doped and $M1$ phase undoped VO₂ thin films, *Phys. Rev. B* **98**, 075152 (2018).
- [6] Y. Zhou and S. Ramanathan, Mott memory and neuromorphic devices, *Proc. IEEE* **103**, 1289 (2015).
- [7] D. Ruzmetov, G. Gopalakrishnan, C. Ko, V. Narayanamurti, and S. Ramanathan, Three-terminal field effect devices utilizing thin film vanadium oxide as the channel layer, *J. Appl. Phys.* **107**, 114516 (2010).

- [8] H.-T. Kim, B.-G. Chae, D.-H. Youn, S.-L. Maeng, G. Kim, K.-Y. Kang, and Y.-S. Lim, Mechanism and observation of mott transition in VO₂-based two-and three-terminal devices, *New J. Phys.* **6**, 52 (2004).
- [9] D. Wegkamp, M. Herzog, L. Xian, M. Gatti, P. Cudazzo, C. L. McGahan, R. E. Marvel, R. F. Haglund Jr, A. Rubio, M. Wolf *et al.*, Instantaneous Band Gap Collapse in Photoexcited Monoclinic VO₂ Due to Photocarrier Doping, *Phys. Rev. Lett.* **113**, 216401 (2014).
- [10] Y. Muraoka, H. Nagao, S. Katayama, T. Wakita, M. Hirai, T. Yokoya, H. Kumigashira, and M. Oshima, Persistent insulator-to-metal transition of a VO₂ thin film induced by soft x-ray irradiation, *Jpn. J. Appl. Phys.* **53**, 05FB09 (2014).
- [11] N. B. Aetukuri, A. X. Gray, M. Drouard, M. Cossale, L. Gao, A. H. Reid, R. Kukreja, H. Ohldag, C. A. Jenkins, E. Arenholz *et al.*, Control of the metal–insulator transition in vanadium dioxide by modifying orbital occupancy, *Nat. Phys.* **9**, 661 (2013).
- [12] Y. Muraoka and Z. Hiroi, Metal–insulator transition of VO₂ thin films grown on TiO₂ (001) and (110) substrates, *Appl. Phys. Lett.* **80**, 583 (2002).
- [13] Z. Tao, Tzong-Ru T. Han, S. D. Mahanti, P. M. Duxbury, F. Yuan, C.-Y. Ruan, K. Wang, and J. Wu, Decoupling of Structural and Electronic Phase Transitions in VO₂, *Phys. Rev. Lett.* **109**, 166406 (2012).
- [14] M. Nakano, K. Shibuya, D. Okuyama, T. Hatano, S. Ono, M. Kawasaki, Y. Iwasa, and Y. Tokura, Collective bulk carrier delocalization driven by electrostatic surface charge accumulation, *Nature (London)* **487**, 459 (2012).
- [15] P. Chaddah, *First Order Phase Transitions of Magnetic Materials: Broad and Interrupted Transitions* (CRC Press, Boca Raton, 2017).
- [16] T. Hanaguri, C. Lupien, Y. Kohsaka, D.-H. Lee, M. Azuma, M. Takano, H. Takagi, and J. Davis, A ‘checkerboard’ electronic crystal state in lightly hole-doped Ca_{2-x}Na_xCuO₂Cl₂, *Nature (London)* **430**, 1001 (2004).
- [17] M. Vershinin, S. Misra, S. Ono, Y. Abe, Y. Ando, and A. Yazdani, Local ordering in the pseudogap state of the high-*T_c* superconductor Bi₂Sr₂CaCu₂O₈ + δ , *Science* **303**, 1995 (2004).
- [18] L. Zhang, C. Israel, A. Biswas, R. Greene, and A. De Lozanne, Direct observation of percolation in a manganite thin film, *Science* **298**, 805 (2002).
- [19] K. Lai, M. Nakamura, W. Kundhikanjana, M. Kawasaki, Y. Tokura, M. A. Kelly, and Z.-X. Shen, Mesoscopic percolating resistance network in a strained manganite thin film, *Science* **329**, 190 (2010).
- [20] J. Dho, Y. Kim, Y. Hwang, J. Kim, and N. Hur, Strain-induced magnetic stripe domains in La_{0.7}Sr_{0.3}MnO₃ thin films, *Appl. Phys. Lett.* **82**, 1434 (2003).
- [21] M. K. Liu, M. Wagner, E. Abreu, S. Kittiwatanakul, A. McLeod, Z. Fei, M. Goldflam, S. Dai, M. M. Fogler, J. Lu, S. A. Wolf, R. D. Averitt, and D. N. Basov, Anisotropic Electronic State via Spontaneous Phase Separation in Strained Vanadium Dioxide Films, *Phys. Rev. Lett.* **111**, 096602 (2013).
- [22] A. Frenzel, M. M. Qazilbash, M. Brehm, B.-G. Chae, B.-J. Kim, H.-T. Kim, A. V. Balatsky, F. Keilmann, and D. N. Basov, Inhomogeneous electronic state near the insulator-to-metal transition in the correlated oxide VO₂, *Phys. Rev. B* **80**, 115115 (2009).
- [23] M. Liu, M. Wagner, J. Zhang, A. McLeod, S. Kittiwatanakul, Z. Fei, E. Abreu, M. Goldflam, A. J. Sternbach, S. Dai *et al.*, Symmetry breaking and geometric confinement in VO₂: Results from a three-dimensional infrared nano-imaging, *Appl. Phys. Lett.* **104**, 121905 (2014).
- [24] A. McLeod, E. Van Heumen, J. Ramirez, S. Wang, T. Saerbeck, S. Guenon, M. Goldflam, L. Andereg, P. Kelly, A. Mueller *et al.*, Nanotextured phase coexistence in the correlated insulator V₂O₃, *Nat. Phys.* **13**, 80 (2017).
- [25] T. Bar, S. K. Choudhary, M. A. Ashraf, K. S. Sujith, S. Puri, S. Raj, and B. Bansal, Kinetic Spinodal Instabilities in the Mott Transition in V₂O₃: Evidence from Hysteresis Scaling and Dissipative Phase Ordering, *Phys. Rev. Lett.* **121**, 045701 (2018).
- [26] M. K. Chattopadhyay, S. B. Roy, A. K. Nigam, K. J. S. Sokhey, and P. Chaddah, Metastability and giant relaxation across the ferromagnetic to antiferromagnetic transition in Ce(Fe_{0.96}Ru_{0.04})₂, *Phys. Rev. B* **68**, 174404 (2003).
- [27] A. Banerjee, P. Chaddah, S. Dash, K. Kumar, A. Lakhani, X. Chen, and R. V. Ramanujan, History-dependent nucleation and growth of the martensitic phase in the magnetic shape memory alloy Ni₄₅Co₅Mn₃₈Sn₁₂, *Phys. Rev. B* **84**, 214420 (2011).
- [28] P. Kushwaha, A. Lakhani, R. Rawat, and P. Chaddah, Low-temperature study of field-induced antiferromagnetic-ferromagnetic transition in Pd-doped Fe-Rh, *Phys. Rev. B* **80**, 174413 (2009).
- [29] P. Levy, F. Parisi, L. Granja, E. Indelicato, and G. Polla, Novel Dynamical Effects and Persistent Memory in Phase Separated Manganites, *Phys. Rev. Lett.* **89**, 137001 (2002).
- [30] C. Liu, E. E. Ferrero, F. Puosi, J.-L. Barrat, and K. Martens, Driving Rate Dependence of Avalanche Statistics and Shapes at the Yielding Transition, *Phys. Rev. Lett.* **116**, 065501 (2016).
- [31] F.-J. Pérez-Reche, B. Tadić, L. Mañosa, A. Planes, and E. Vives, Driving Rate Effects in Avalanche-Mediated First-Order Phase Transitions, *Phys. Rev. Lett.* **93**, 195701 (2004).
- [32] F. Zhong, Renormalization-group theory of first-order phase transition dynamics in field-driven scalar model, *Front. Phys.* **12**, 126402 (2017).
- [33] F. Zhong and Q. Chen, Theory of the Dynamics of First-Order Phase Transitions: Unstable Fixed Points, Exponents, and Dynamical Scaling, *Phys. Rev. Lett.* **95**, 175701 (2005).
- [34] S. S. Majid, S. R. Sahu, A. Ahad, K. Dey, K. Gautam, F. Rahman, P. Behera, U. Deshpande, V. Sathe, and D. K. Shukla, Role of vv dimerization in the insulator-metal transition and optical transmittance of pure and doped VO₂ thin films, *Phys. Rev. B* **101**, 014108 (2020).
- [35] See Supplemental Material at <http://link.aps.org/supplemental/10.1103/PhysRevB.107.134106> for details of characterizations by using x-ray diffraction, Raman spectroscopy, resistivity, minor hysteresis loop measurements, frequency and FWHM vs temperature behavior of Raman modes, Raman mapping, x-ray absorption spectroscopy, evaluations of parameters influencing Raman spectra, thermal hysteresis scaling in bulk VO₂ and V₂O₃, and time-domain thermoreflectance spectra of the VO₂ thin film.
- [36] P. Schilbe and D. Maurer, Lattice dynamics in VO₂ near the metal-insulator transition, *Materials Science and Engineering: A* **370**, 449 (2004).

- [37] C. Marini, E. Arcangeletti, D. Di Castro, L. Baldassare, A. Perucchi, S. Lupi, L. Malavasi, L. Boeri, E. Pomjakushina, K. Conder, and P. Postorino, Optical properties of $V_{1-x}Cr_xO_2$ compounds under high pressure, *Phys. Rev. B* **77**, 235111 (2008).
- [38] F. Ureña-Begara, A. Crunteanu, and J.-P. Raskin, Raman and XPS characterization of vanadium oxide thin films with temperature, *Appl. Surf. Sci.* **403**, 717 (2017).
- [39] C. Tatsuyama and H. Fan, Raman scattering and phase transitions in V_2O_3 and $(V_{1-x}Cr_x)_2O_3$, *Phys. Rev. B* **21**, 2977 (1980).
- [40] S. Lee, I. N. Ivanov, J. K. Keum, and H. N. Lee, Epitaxial stabilization and phase instability of VO_2 polymorphs, *Sci. Rep.* **6**, 19621 (2016).
- [41] K. Shibuya and A. Sawa, Polarized raman scattering of epitaxial vanadium dioxide films with low-temperature monoclinic phase, *J. Appl. Phys.* **122**, 015307 (2017).
- [42] D. Lee, D. Yang, H. Kim, J. Kim, S. Song, K. S. Choi, J.-S. Bae, J. Lee, J. Lee, Y. Lee *et al.*, Deposition-temperature-mediated selective phase transition mechanism of VO_2 films, *J. Phys. Chem. C* **124**, 17282 (2020).
- [43] Y. Ho, C. Chang, D. Wei, C. Dong, C. Chen, J. Chen, W. Jang, C. Hsu, T. Chan, K. Kumar *et al.*, Characterization of gasochromic vanadium oxides films by x-ray absorption spectroscopy, *Thin Solid Films* **544**, 461 (2013).
- [44] M. Abbate, H. Pen, M. Czyżyk, F. De Groot, J. Fuggle, Y. Ma, C. Chen, F. Sette, A. Fujimori, Y. Ueda *et al.*, Soft x-ray absorption spectroscopy of vanadium oxides, *J. Electron Spectrosc. Relat. Phenom.* **62**, 185 (1993).
- [45] D. S. Su and R. Schlögl, Thermal decomposition of divanadium pentoxide V_2O_5 : Towards a nanocrystalline V_2O_3 phase, *Catal. Lett.* **83**, 115 (2002).
- [46] L. Yeo, A. Srivastava, M. Majidi, R. Sutarto, F. He, S. Poh, C. Diao, X. Yu, M. Motapothula, S. Saha *et al.*, Anomalous spectral-weight transfers unraveling oxygen screening and electronic correlations in the insulator-metal transition of VO_2 , *Phys. Rev. B* **91**, 081112 (2015).
- [47] S. Zhang, B. Shang, J. Yang, W. Yan, S. Wei, and Y. Xie, From VO_2 (b) to VO_2 (a) nanobelts: First hydrothermal transformation, spectroscopic study and first principles calculation, *Phys. Chem. Chem. Phys.* **13**, 15873 (2011).
- [48] J. Ortin, Preisach modeling of hysteresis for a pseudoelastic Cu-Zn-Al single crystal, *J. Appl. Phys.* **71**, 1454 (1992).
- [49] P. Jung, G. Gray, R. Roy, and P. Mandel, Scaling Law for Dynamical Hysteresis, *Phys. Rev. Lett.* **65**, 1873 (1990).
- [50] G. Zheng and J. Zhang, Thermal hysteresis scaling for first-order phase transitions, *J. Phys.: Condens. Matter* **10**, 275 (1998).
- [51] S. B. Roy, First order magneto-structural phase transition and associated multi-functional properties in magnetic solids, *J. Phys.: Condens. Matter* **25**, 183201 (2013).
- [52] S. Yesudhas, R. Burns, B. Lavina, S. N. Tkachev, J. Sun, C. A. Ullrich, and S. Guha, Coupling of organic cation and inorganic lattice in methylammonium lead halide perovskites: Insights into a pressure-induced isostructural phase transition, *Phys. Rev. Mater.* **4**, 105403 (2020).
- [53] S. Yesudhas, N. Yedukondalu, M. K. Jana, J. Zhang, J. Huang, B. Chen, H. Deng, R. Sereika, H. Xiao, S. Sinogeikin *et al.*, Structural, vibrational, and electronic properties of 1D-TiInTe₂ under high pressure: A combined experimental and theoretical study, *Inorg. Chem.* **60**, 9320 (2021).
- [54] E. Evlyukhin, S. A. Howard, H. Paik, G. J. Paez, D. J. Gosztola, C. N. Singh, D. G. Schlom, W.-C. Lee, and L. F. Piper, Directly measuring the structural transition pathways of strain-engineered VO_2 thin films, *Nanoscale* **12**, 18857 (2020).
- [55] S. Zhang, J. Y. Chou, and L. J. Lauhon, Direct correlation of structural domain formation with the metal insulator transition in a VO_2 nanobeam, *Nano Lett.* **9**, 4527 (2009).
- [56] E. Evlyukhin, E. Kim, D. Goldberger, P. Cifligu, S. Schyck, P. F. Weck, and M. Pravica, High-pressure-assisted x-ray-induced damage as a new route for chemical and structural synthesis, *Phys. Chem. Chem. Phys.* **20**, 18949 (2018).
- [57] K. Okimura, N. Hanis Azhan, T. Hajiri, S.-i. Kimura, M. Zaghrioui, and J. Sakai, Temperature-dependent raman and ultraviolet photoelectron spectroscopy studies on phase transition behavior of VO_2 films with M1 and M2 phases, *J. Appl. Phys.* **115**, 153501 (2014).
- [58] G. Petrov, V. Yakovlev, and J. Squier, Raman microscopy analysis of phase transformation mechanisms in vanadium dioxide, *Appl. Phys. Lett.* **81**, 1023 (2002).
- [59] M. Yang, Y. Yang, B. Hong, L. Wang, K. Hu, Y. Dong, H. Xu, H. Huang, J. Zhao, H. Chen *et al.*, Suppression of structural phase transition in VO_2 by epitaxial strain in vicinity of metal-insulator transition, *Sci. Rep.* **6**, 23119 (2016).
- [60] M. Nazari, Y. Zhao, V. V. Kuryatkov, Z. Fan, A. A. Bernussi, and M. Holtz, Temperature dependence of the optical properties of VO_2 deposited on sapphire with different orientations, *Phys. Rev. B* **87**, 035142 (2013).
- [61] Y. Huang, D. Zhang, Y. Liu, J. Jin, Y. Yang, T. Chen, H. Guan, P. Fan, and W. Lv, Phase transition analysis of thermochromic VO_2 thin films by temperature-dependent raman scattering and ellipsometry, *Appl. Surf. Sci.* **456**, 545 (2018).
- [62] D. G. Cahill, Analysis of heat flow in layered structures for time-domain thermoreflectance, *Rev. Sci. Instrum.* **75**, 5119 (2004).
- [63] W.-P. Hsieh, B. Chen, J. Li, P. Keblinski, and D. G. Cahill, Pressure tuning of the thermal conductivity of the layered muscovite crystal, *Phys. Rev. B* **80**, 180302 (2009).
- [64] X. Zheng, D. Cahill, P. Krasnochtchekov, R. Averback, and J.-C. Zhao, High-throughput thermal conductivity measurements of nickel solid solutions and the applicability of the wiedemann–franz law, *Acta Mater.* **55**, 5177 (2007).
- [65] D.-W. Oh, C. Ko, S. Ramanathan, and D. G. Cahill, Thermal conductivity and dynamic heat capacity across the metal-insulator transition in thin film VO_2 , *Appl. Phys. Lett.* **96**, 151906 (2010).
- [66] S. Lee, K. Hippalgaonkar, F. Yang, J. Hong, C. Ko, J. Suh, K. Liu, K. Wang, J. J. Urban, X. Zhang *et al.*, Anomalously low electronic thermal conductivity in metallic vanadium dioxide, *Science* **355**, 371 (2017).
- [67] J. W. Christian, *The theory of transformations in metals and alloys* (Newnes, Oxford, 2002).
- [68] R. M. White and T. H. Geballe, *Long Range Order in Solids: Solid State Physics* (Academic Press, Cambridge, Massachusetts, 2013).
- [69] M. Manekar and S. Roy, Nucleation and growth dynamics across the antiferromagnetic to ferromagnetic transition in $(Fe_{0.975}Ni_{0.025})_{50}Rh_{50}$: Analogy with crystallization, *J. Phys.: Condens. Matter* **20**, 325208 (2008).
- [70] J. Y. Suh, R. Lopez, L. C. Feldman, and R. Haglund Jr, Semiconductor to metal phase transition in the nucleation and growth

- of VO₂ nanoparticles and thin films, *J. Appl. Phys.* **96**, 1209 (2004).
- [71] T. J. Huffman, D. J. Lahneman, S. L. Wang, T. Slusar, B.-J. Kim, H.-T. Kim, and M. M. Qazilbash, Highly repeatable nanoscale phase coexistence in vanadium dioxide films, *Phys. Rev. B* **97**, 085146 (2018).
- [72] K. H. Ahn, T. Lookman, and A. Bishop, Strain-induced metal-insulator phase coexistence in perovskite manganites, *Nature (London)* **428**, 401 (2004).
- [73] P. H. M. S. S. Pierre Papon, Jacques Leblond, *The Physics of Phase Transitions. Concepts and Applications*, 2nd ed. (Springer, Berlin Heidelberg, 2010).